

# Power Time Series Forecasting by Pretrained LM

Tian Zhou<sup>\*1</sup> Peisong Niu<sup>\*1</sup> Xue Wang<sup>\*2</sup> Liang Sun<sup>2</sup> Rong Jin<sup>2</sup>

## Abstract

The diversity and domain dependence of time series data pose significant challenges in transferring learning to time series forecasting. In this study, we examine the effectiveness of using a transformer model that has been pre-trained on natural language or image data and then fine-tuned for time series forecasting with minimal modifications, specifically, without altering the self-attention and feedforward layers of the residual blocks. This model, known as the Frozen Pre-trained Transformer (FPT), is evaluated through fine-tuning on time series forecasting tasks under Zero-Shot, Few-Shot, and normal sample size conditions. Our results demonstrate that pre-training on natural language or images can lead to a comparable or state-of-the-art performance in cross-modality time series forecasting tasks, in contrast to previous studies that focused on fine-tuning within the same modality as the pre-training data. Additionally, we provide a comprehensive theoretical analysis of the universality and the functionality of the FPT. The code is publicly available at <https://anonymous.4open.science/r/Pretrained-LM-for-TSForecasting-C561>.

## 1. Introduction

Time series forecasting is a fundamental problem dating back to thousands of years ago (Hyndman & Athanasopoulos, 2021). It has played an important role in numerous real-world applications, such as retail (Böse et al., 2017; Courty & Li, 1999), healthcare (Lim et al., 2018; Zhang & Nawata, 2018), and engineering systems (Zhang et al., 2019; Gonzalez-Vidal et al., 2019). In the literature, many algorithms have been proposed, including classic statistical methods and machine learning algorithms. Recently, numerous deep learning models have shown their power in pro-

cessing sequential data, especially in the area of natural language processing (NLP). Among these deep learning models, the recurrent neural network is probably the most well-examined (Connor et al., 1994; Hewamalage et al., 2021). Following the recent success in natural language process (NLP) and computer vision (CV) communities (Vaswani et al., 2017; Devlin et al., 2019; Dosovitskiy et al., 2021; Rao et al., 2021), Transformer (Vaswani et al., 2017) has been introduced to various time series tasks with promising results (Wen et al., 2022), especially for long-term forecasting (Zhou et al., 2022; 2021; Wu et al., 2021).

One significant challenge limiting the application of deep learning algorithms in time series forecasting is the problem of **insufficient training sample**. It is observed in many applications of time series and not fully addressed, especially in the few-shot learning setting. Similar to time series data, other sequential data is widely observed and studied in natural language processing (NLP) or computer vision (CV) areas. The pretrain-finetune paradigm is widely used in these areas, but it is not widely adopted in the domain of time series, where end-to-end algorithms still dominate various applications. So far, very limited progress has been made for time series, including transfer learning for time series classification (Ismail Fawaz et al., 2018) and in-domain knowledge transfer for time series forecasting (Oreshkin et al., 2021). One reason for this difficulty is the diversity of time series data in different domains. Compared with typical sequential data in NLP and computer vision, time series data is more domain-dependent. For example, the time series of electric load and the time series of CPU usage of a cloud service may have quite different patterns and characteristics. Recently, some researchers have noticed the transfer learning ability of pretrained-transformer models to cross-domain tasks (Lu et al., 2022), but cross-domain knowledge transfer for time series data is even more challenging due to the diversity of time series data in different domains.

In this paper, we propose using pretrained language model to power the time series forecasting in few-shot learning, full data learning, zero-shot learning settings. To the best of our knowledge, this is the first work to investigate the cross-domain knowledge transfer for the time series forecasting task.

<sup>\*</sup>Equal contribution <sup>1</sup>DAMO Academy, Alibaba Group, Hangzhou, China <sup>2</sup>DAMO Academy, Alibaba Group, Bellevue, USA. Correspondence to: Rong Jin <jinrong.jr@alibaba-inc.com>.

Here we summarize our key contributions as follows:

1. We propose using a frozen pretrained language model to achieve a SOTA performance in few-shot learning setting. The effectiveness of our design is justified from both empirical and theoretical perspectives.
2. We demonstrate that our proposed algorithm can achieve a SOTA or comparable result in full data regular time series forecasting tasks and zero-sample forecasting tasks with various recent baseline models.
3. We demonstrate the universality of our approach by exploring the possibility of using a pretrained transformer model from another domain (computer vision) to power the time series forecasting.

The remainder of this paper is structured as follows. In Section 2, we provide a summary of related works relevant to our study. Section 3 presents the proposed detailed model structure. In Section 4, we conduct a thorough evaluation of the performance of cross-domain time series forecasting using a pre-trained language model under a few-shot learning setting, compared to various state-of-the-art baseline models. Section 5 provides a theoretical explanation of the universality and functionality of language models in cross-domain time series forecasting tasks. In Section 6, we demonstrate the state-of-the-art performance of our proposed method under a full-data learning setting and a zero-shot learning setting, and we explore the possibility of using pre-trained models from the computer vision domain. Finally, in Section 7, we discuss our results and future directions.

## 2. Related Work

In this section, we selectively show the related literature for this paper. The relevant works include time series forecasting, in-domain transfer learning, and cross-domain knowledge transfer learning. We put end2end time series forecasting-related works in Appendix A and summarized the most related in-domain and cross-domain transfer learning works.

**In-domain Transfer Learning through pretrained models** In recent years, a large number of research works have verified the effectiveness of the pretrained model from NLP, CV to Vision-and-Language (VL). Latest studies for NLP focus on learning contextual word embeddings for downstream tasks. With the increase of computing power, the very deep transformer models have shown powerful representation ability in various language tasks. Among them, BERT (Devlin et al., 2019) uses transformer encoders and employs masked language modeling task that aims to recover the random masked tokens within a text. OpenAI

proposed GPT (Radford & Narasimhan, 2018) that trains transformer decoders on a large language corpus and then finetunes on task-specific data. GPT2 (Radford et al., 2019) is trained on larger datasets with much more parameters and can be transferred to various downstream tasks. Since transformer models can adapt to various inputs, the idea of pretraining can also be well adapted to visual tasks. DEiT (Touvron et al., 2021) proposed a teacher-student strategy for transformers with convolution neural networks (CNNs) as the teacher model and achieve competitive performance. BEiT (Bao et al., 2022) converts images as visual tokens and successfully uses the BERT model in CV. However, because of the **insufficient training sample**, there is little research work about pretrained models on time series forecasting.

**Cross-domain knowledge transfer** Since transformers can handle different modal tasks through tokenizing the inputs to embeddings, it is also an interesting topic whether the transformers have universal representation ability and can be used for transferring between various domains. The VL pretrained model VLMo (Bao et al., 2021) proposed a stagewise pretraining strategy that utilizes frozen attention blocks pretrained by image-only data to train the language expert. One of the most related works which transfer knowledge from a pretrained language model to other domains is (Lu et al., 2022), which studies the strong performance of a frozen pretrained language model(LM) compared to an end2end transformer alternative learned from other domains’ data. Another relative work for knowledge transfer to the time series domain is the Voice2series (Yang et al., 2021), which leverages a pretrained speech processing model for time series classification and achieves superior performance. To the best of our knowledge, there is no previous work investigating the cross-domain knowledge transfer for the time series forecasting task.

## 3. Methodology

### 3.1. Model Structure

The architecture we employ is depicted in Figure 1. We utilize parameters from NLP pretrained transformer models for time series forecasting, with a focus on the GPT2 model (Radford et al., 2019). We also experiment with other models, such as BERT (Devlin et al., 2019) and BEiT (Bao et al., 2022), to demonstrate the universal performance of cross-domain knowledge transfer in powering time series forecasting.

**Frozen Pretrained Block** The embedding layers and self-attention blocks from the pretrained models are utilized directly in our architecture. Since cross-domain knowledge is advantageous for time series forecasting, we freeze the self-attention blocks. However, the input and output layers are randomly initialized and require training to adapt to a

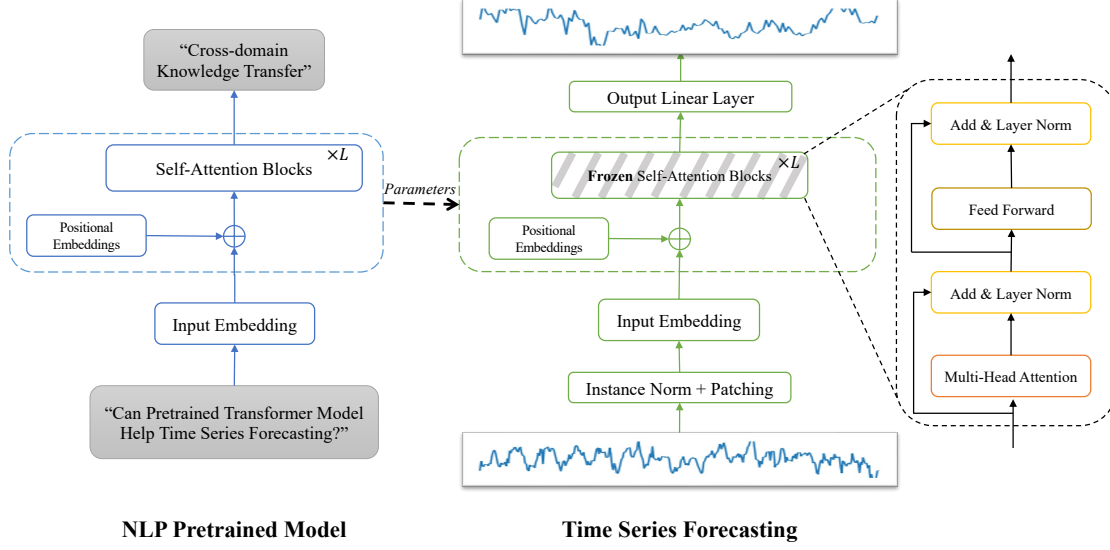


Figure 1. Model architecture. NLP pretrained parameters are transferred to the time series forecasting tasks. Self-attention and Feedforward layers in the transformer blocks are frozen while only the embedding layer, normalization layers, and output layer require training.

new domain.

**Positional Embeddings and Layer Normalization** We fine-tune the positional embeddings and layer normalization layer, as it is a standard practice to bring a small benefit to most downstream tasks (Lu et al., 2022; Housby et al., 2019). Therefore, they require re-training in our architecture.

**Input Embedding** As we aim to apply the NLP pretrained model to a new modality, we must redesign the input embedding layer, which projects the time series data to the required dimensions of the specific pretrained model. We achieve this through linear probing, reducing the number of parameters for training.

**Instance Normalization** Distribution shifts can hinder the accuracy of most time series forecasting methods. We utilize reversible instance normalization (Kim et al., 2022) to address this issue, which normalizes the input time series with mean and variance, and then adds them back to the output.

**Patching** We employ patching (Nie et al., 2022) to extract local semantic information by aggregating adjacent time steps, forming a single patch-based token. Patching significantly increases the input historical time horizon while maintaining the same token length and reducing information redundancy for the transformer models. In our architecture, we apply patching after instance normalization.

## 4. Main Experiments

To evaluate the time series representation ability of the GPT2-backbone FPT model, we evaluate few-shot learning tasks. Then, a justification is given to provide a theoretical understanding of why a pretrained LM can be effective in time-series forecasting. Moreover, a diverse of analytical experiments are performed to gain a clearer understanding of how architecture works on time series forecasting. We also present experiments on BERT-backbone FPT (Devlin et al., 2019) model and more importantly the image-pretrained BEiT-backbone FPT model (Bao et al., 2022) to illustrate the performance of the proposed architecture is not limited to GPT2 model and NLP domain. Finally, we investigate representation ability in zero-shot transfer learning. In this section, We mainly use the results of the GPT2-backbone (6 Layers) FPT model, that only the first 6 layers of GPT2 are reserved, for comparison with baseline algorithms.

### 4.1. Few-shot Learning

We first define a novel few-shot time series forecasting task and test different algorithms on six popular real-world datasets, including weather, ILI, and 4 ETT datasets (ETTh1, ETTh2, ETTm1, ETTm2). We use the most recently published methods, DLinear (Zeng et al., 2023), PatchTST (Nie et al., 2022), FEDformer (Zhou et al., 2022) and Autoformer (Wu et al., 2021), as our baselines. Note that since PatchTST holds the best performance in all transformer models and DLinear can also outperform most transformer models for underfit with long look-back windows, they are used as the main SOTA baseline models for comparison.

Table 1. Few-shot learning results on 5% data. We use prediction length  $O \in \{96, 192, 336, 720\}$  for ILI and  $O \in \{24, 36, 48, 60\}$  for others. A lower MSE indicates better performance, and the best results are highlighted in bold. '-' means that 5% time series is not sufficient to constitute a training set. GPT2(6) and GPT2(0) represent GPT2-backbone 6 layers model and 0 layer model respectively

Methods		GPT2(6)		GPT2(0)		DLinear		PatchTST		FEDformer		Autoformer	
Metric		MSE	MAE	MSE	MAE	MSE	MAE	MSE	MAE	MSE	MAE	MSE	MAE
Weather	96	0.175	<b>0.230</b>	0.191	0.243	0.184	0.242	<b>0.171</b>	0.224	0.229	0.309	0.227	0.299
	192	<b>0.227</b>	<b>0.276</b>	0.244	0.289	0.228	0.283	0.230	0.277	0.265	0.317	0.278	0.333
	336	0.286	<b>0.322</b>	0.303	0.332	<b>0.279</b>	<b>0.322</b>	0.294	0.326	0.353	0.392	0.351	0.393
	720	0.366	<b>0.379</b>	0.391	0.393	<b>0.364</b>	0.388	0.384	0.387	0.391	0.394	0.387	0.389
ETTh1	96	<b>0.543</b>	0.506	0.825	0.638	0.547	<b>0.503</b>	0.557	0.519	0.593	0.529	0.681	0.570
	192	0.748	0.580	1.220	0.778	0.720	0.604	0.711	0.570	<b>0.652</b>	<b>0.563</b>	0.725	0.602
	336	0.754	0.595	1.852	0.965	0.984	0.727	0.816	0.619	<b>0.731</b>	<b>0.594</b>	0.761	0.624
	720	-	-	-	-	-	-	-	-	-	-	-	-
ETTh2	96	<b>0.376</b>	<b>0.421</b>	0.551	0.507	0.442	0.456	0.401	0.421	0.390	0.424	0.428	0.468
	192	<b>0.418</b>	<b>0.441</b>	0.765	0.610	0.617	0.542	0.452	0.455	0.457	0.465	0.496	0.504
	336	<b>0.408</b>	<b>0.439</b>	0.767	0.614	1.424	0.849	0.464	0.469	0.477	0.483	0.486	0.496
	720	-	-	-	-	-	-	-	-	-	-	-	-
ETTm1	96	0.386	0.405	0.582	0.512	<b>0.332</b>	<b>0.374</b>	0.399	0.414	0.628	0.544	0.726	0.578
	192	0.440	0.438	0.632	0.536	<b>0.358</b>	<b>0.390</b>	0.441	0.436	0.666	0.566	0.750	0.591
	336	0.485	0.459	0.767	0.584	<b>0.402</b>	<b>0.416</b>	0.499	0.467	0.807	0.628	0.851	0.659
	720	0.577	0.499	1.334	0.742	<b>0.511</b>	<b>0.489</b>	0.767	0.587	0.822	0.633	0.857	0.655
ETTm2	96	<b>0.199</b>	<b>0.280</b>	0.282	0.347	0.236	0.326	0.206	0.288	0.229	0.320	0.232	0.322
	192	<b>0.256</b>	<b>0.316</b>	0.346	0.383	0.306	0.373	0.264	0.324	0.394	0.361	0.291	0.357
	336	<b>0.318</b>	<b>0.353</b>	0.429	0.427	0.380	0.423	0.334	0.367	0.378	0.427	0.478	0.517
	720	0.460	0.436	0.751	0.568	0.674	0.583	<b>0.454</b>	<b>0.432</b>	0.523	0.510	0.553	0.538
ECL	96	<b>0.143</b>	<b>0.241</b>	0.147	0.246	0.150	0.251	0.145	0.244	0.235	0.322	0.297	0.367
	192	<b>0.159</b>	<b>0.255</b>	0.163	0.260	0.163	0.263	0.163	0.260	0.247	0.341	0.308	0.375
	336	<b>0.179</b>	<b>0.274</b>	0.182	0.278	0.175	0.278	0.183	0.281	0.267	0.356	0.354	0.411
	720	0.233	0.323	0.239	0.329	<b>0.219</b>	<b>0.311</b>	0.233	0.323	0.318	0.394	0.426	0.466
Traf fic	96	0.419	0.298	0.468	0.354	0.427	0.304	<b>0.404</b>	<b>0.286</b>	0.670	0.421	0.795	0.481
	192	0.434	0.305	0.479	0.352	0.447	0.315	<b>0.412</b>	<b>0.294</b>	0.653	0.405	0.837	0.503
	336	0.449	0.313	0.477	0.345	0.478	0.333	<b>0.439</b>	<b>0.310</b>	0.707	0.445	0.867	0.523
	720	-	-	-	-	-	-	-	-	-	-	-	-
Count		11	13	0	0	7	6	6	5	2	2	0	0

**Task Definition** Since (Zeng et al., 2023) and (Nie et al., 2022) have verified that channel-independence works in the above datasets, we directly treat multivariate series as univariate series. Similar to traditional experimental settings, each time series is split into three parts: training data, validation data, and test data. For the few-shot forecasting task, only a certain percentage (5%, 10%) timesteps of training data are kept, and the other two parts remain unchanged. The evaluation metrics remain the same as for classic multivariate time series forecasting. We repeat this experiment 3 times and report the average metrics in the following experiments.

## Key Results

For each dataset, we also compare our results to GPT2-backbone (0 Layers) FPT which is GPT2 without any attention blocks reserved. The results of 5% and 10% few-shot learning are shown in Table 1 and Table 2. Compared with GPT2-backbone (0 Layers) FPT, GPT2-backbone (6 Layers) FPT yields overall **31.6%** relative MSE reduction on 5% data and **25.4%** relative MSE reduction on 10% data. Compared to the state of art methods DLinear and PatchTST, GPT2-backbone (6 Layers) FPT achieves the most winning counts on both 5% data and 10% data. It verifies that NLP

pretrained attention and cross-domain transfer knowledge can be effectively applied to time series forecasting. A subset of mean and standard deviation (STD) results are provided in Appendix C.2.

## 5. Theoretical Justification

In this context, we aim to tackle two primary questions:

1. What is the source of universality that enables a language model, trained on natural language token distributions, to perform cross-domain time series forecasting tasks with high efficiency?
2. What is the actual function of a frozen pretrained model in time series forecasting tasks?

### 5.1. Universality

Our first question is: why does the proposed pretrained-frozen-model work so effectively? We have achieved state-of-the-art performance in time series forecasting using a language model that is mostly trained on natural language data. The answer lies in the universality of the frozen structure, which includes attention layers and Feed Forward layers.

Table 2. Few-shot learning results on 10% data. We use prediction length  $O \in \{96, 192, 336, 720\}$  for ILI and  $O \in \{24, 36, 48, 60\}$  for others. A lower MSE indicates better performance, and the best results are highlighted in bold. '-' means that 10% time series is not sufficient to constitute a training set. GPT2(6) and GPT2(0) represent GPT2-backbone 6 layers model and 0 layer model respectively.

Methods		GPT2(6)		GPT2(0)		DLinear		PatchTST		FEDformer		Autoformer	
Metric		MSE	MAE	MSE	MAE	MSE	MAE	MSE	MAE	MSE	MAE	MSE	MAE
Weather	96	<b>0.163</b>	<b>0.215</b>	0.190	0.240	0.171	0.224	0.165	0.215	0.188	0.253	0.221	0.297
	192	<b>0.210</b>	<b>0.254</b>	0.243	0.284	0.215	0.263	0.210	0.257	0.250	0.304	0.270	0.322
	336	<b>0.256</b>	<b>0.292</b>	0.270	0.305	0.258	0.299	0.259	0.297	0.312	0.346	0.320	0.351
	720	0.321	<b>0.339</b>	0.348	0.359	<b>0.320</b>	0.346	0.332	0.346	0.387	0.393	0.390	0.396
ETTh1	96	<b>0.458</b>	<b>0.456</b>	0.601	0.536	0.492	0.495	0.516	0.485	0.512	0.499	0.613	0.552
	192	0.570	<b>0.516</b>	0.709	0.587	<b>0.565</b>	0.538	0.598	0.524	0.624	0.555	0.722	0.598
	336	<b>0.608</b>	<b>0.535</b>	0.801	0.635	0.721	0.622	0.657	0.550	0.691	0.574	0.750	0.619
	720	0.725	<b>0.591</b>	1.385	0.831	0.986	0.743	0.762	0.610	0.728	0.614	<b>0.721</b>	0.616
ETTh2	96	<b>0.331</b>	<b>0.374</b>	0.539	0.495	0.357	0.411	0.353	0.389	0.382	0.416	0.413	0.451
	192	<b>0.402</b>	<b>0.411</b>	0.675	0.555	0.569	0.519	0.403	0.414	0.478	0.474	0.474	0.477
	336	<b>0.406</b>	<b>0.433</b>	0.718	0.580	0.671	0.572	0.426	0.441	0.504	0.501	0.547	0.543
	720	<b>0.449</b>	<b>0.464</b>	0.732	0.605	0.824	0.648	0.477	0.480	0.499	0.509	0.516	0.523
ETTm1	96	0.390	0.404	0.610	0.508	<b>0.352</b>	<b>0.392</b>	0.410	0.419	0.578	0.518	0.774	0.614
	192	0.429	0.423	0.666	0.540	<b>0.382</b>	<b>0.412</b>	0.437	0.434	0.617	0.546	0.754	0.592
	336	0.469	0.439	0.895	0.615	<b>0.419</b>	<b>0.434</b>	0.476	0.454	0.998	0.775	0.869	0.677
	720	0.569	0.498	0.916	0.646	<b>0.490</b>	<b>0.477</b>	0.681	0.556	0.693	0.579	0.810	0.630
ETTm2	96	<b>0.188</b>	<b>0.269</b>	0.283	0.344	0.213	0.303	0.191	0.274	0.291	0.399	0.352	0.454
	192	<b>0.251</b>	<b>0.309</b>	0.353	0.384	0.278	0.345	0.252	0.317	0.307	0.379	0.694	0.691
	336	0.307	<b>0.346</b>	0.420	0.422	0.338	0.385	<b>0.306</b>	0.353	0.543	0.559	2.408	1.407
	720	<b>0.426</b>	<b>0.417</b>	0.553	0.491	0.436	0.440	0.433	0.427	0.712	0.614	1.913	1.166
ILI	24	<b>3.022</b>	<b>1.247</b>	3.521	1.274	3.969	1.536	3.144	1.261	4.338	1.525	3.733	1.380
	36	3.854	1.453	3.466	1.340	3.700	1.467	<b>2.950</b>	<b>1.237</b>	5.166	1.658	4.342	1.507
	48	4.603	1.571	4.435	1.554	3.980	1.485	3.501	1.358	4.404	1.523	4.267	1.493
	60	-	-	-	-	-	-	-	-	4.380	<b>1.498</b>	<b>4.429</b>	1.527
ECL	96	<b>0.139</b>	<b>0.237</b>	0.142	0.240	0.150	0.253	0.140	0.238	0.231	0.323	0.261	0.348
	192	<b>0.156</b>	<b>0.252</b>	0.158	0.254	0.164	0.264	0.160	0.255	0.261	0.356	0.338	0.406
	336	<b>0.175</b>	<b>0.270</b>	<b>0.175</b>	0.271	0.181	0.282	0.180	0.276	0.360	0.445	0.410	0.474
	720	0.233	0.317	0.230	<b>0.315</b>	<b>0.223</b>	0.321	0.241	0.323	0.530	0.585	0.715	0.685
Traffic	96	0.414	0.297	0.478	0.368	0.419	0.298	<b>0.403</b>	<b>0.289</b>	0.639	0.400	0.672	0.405
	192	0.426	0.301	0.481	0.363	0.434	0.305	<b>0.415</b>	<b>0.296</b>	0.637	0.416	0.727	0.424
	336	0.434	<b>0.303</b>	0.488	0.365	0.449	0.313	<b>0.426</b>	0.304	0.655	0.427	0.749	0.454
	720	0.487	0.337	0.537	0.386	0.484	0.336	<b>0.474</b>	<b>0.331</b>	0.722	0.456	0.847	0.499
Count		16	21	1	1	7	4	6	4	0	1	1	0

To gain a better understanding, let's start by examining a "zero-layer" Transformer model. This model operates by taking a token, embedding it, and transforming it back to produce logits that predict the subsequent token. Because it cannot transfer information from other tokens, it relies solely on the current token to predict the next one. Consequently, the optimal behavior of this model is to closely resemble the **bigram** log-likelihood.

Then we move on to the so-called "attention-only" transformer, which doesn't have MLP layers. As discussed in a recent work (Elhage et al., 2021), one-layer attention-only Transformers can be comprehended as a combination of a **bigram** model and multiple "skip-trigram" models (impacting the probabilities of sequences "A... BC"). This can be intuitively understood as each attention head having the ability to selectively attend from the current token ("B") to a previous token ("A") and transfer relevant information to fine-tune the probability of potential subsequent tokens ("C"). (Olsson et al., 2022) further discusses a multi-layer transformer can do more complex n-gram estimation using

an induction heads mechanism. To be more precise, induction heads employ a straightforward principle: the '[A][B] ... [A] → [B]' rule, which elevates the likelihood of generating the subsequent token 'B' given the current token 'A' if there is a fuzzy match of the AB bigram in the historical context. This rule seems to largely decouple A and B, which means they do not memorize a fixed table of n-gram statistics. The rule [A][B] ... [A] → [B] applies regardless of what A and B are, which can abstract to new patterns.

Building upon these discussions, we are now prepared to substantiate the following argument: **For sequential data following a power law, there is a potentially universal solution to the final estimation of n-gram probabilities.** That's the reason behind the universality of pretrained LM's performance in cross-domain tasks. For simplicity, we assume that  $n$  is so large that we are unable to observe any occurrence of  $n$ -gram from data, and we only observe the occurrence of  $n'$ -grams with  $n' < n$ . We denote by  $s_i^n$  the  $i$ th unique  $n$ -gram, and by the notation  $s_j^{n'} \in s_i^n$  if  $n'$ -gram  $s_j^{n'}$  appears in  $s_i^n$ , the  $i$ th  $n$ -gram. Let  $m_n$  be the number of



unique  $n$ -grams. According to the maximum entropy model, our estimation of  $n$ -gram probabilities can be cast into the following optimization problem:

$$\min \sum_{i=1}^{m_n} p(s_i^n) \log p(s_i^n) \quad \text{s. t.} \quad \sum_{i: s_j^{n'} \in s_i^n} p(s_i^n) = \hat{p}(s_j^{n'}),$$

where  $\hat{p}(s_j^{n'})$  represents the probability of observing pattern  $s_j^{n'}$  from the data and  $j \in [m_{n'}]$ ,  $n' \in [n-1]$ .

For each constraint for  $\hat{p}(s_j^{n'})$ , we introduce a Lagrangian dual variable  $\lambda_j^{n'}$ , and rewrite the optimization problem as follows

$$\min_{\lambda} \log \left( \sum_{i=1}^{m_n} \exp \left( \sum_{(n',j): s_j^{n'} \in s_i^n} \lambda_j^{n'} \right) \right) - \sum_{n'=1}^{n-1} \sum_{j=1}^{m_{n'}} \lambda_j^{n'} \hat{p}(s_j^{n'}),$$

where  $n$ -gram probability  $p(s_j^n)$  is given as  $p(s_j^n) = \frac{1}{Z(\lambda)} \exp(\sum_{(n',j): s_j^{n'} \in s_i^n} \lambda_j^{n'})$  and  $Z(\lambda) = \sum_{i=1}^{m_n} \exp(\sum_{(n',j): s_j^{n'} \in s_i^n} \lambda_j^{n'})$

In the case that all  $n$ -grams follow a power law, for each  $n' \in [n-1]$ , we divide  $n'$ -gram into two groups: the group  $\mathcal{V}_{n'}$  includes the high frequency  $n'$ -gram and the group  $\mathcal{U}_{n'}$  including the low frequency of  $n'$ -gram. For simplicity, we assume that the probability for all the high frequency  $n'$ -grams are roughly  $\alpha_{n'} \in [0, 1]$  and the probability for all the low frequency  $n'$ -grams are roughly  $\beta_{n'} \in [0, 1]$ . By assuming that all the patterns in  $\mathcal{V}_{n'}$  and  $\mathcal{U}_{n'}$  share similar appearance frequency, we simplify the optimization problem by only introducing two dual variables for each  $n'$ -gram, i.e.  $\lambda_a^{n'}$  for high-frequency patterns and  $\lambda_b^{n'}$  for low-frequency patterns as follow

$$\begin{aligned} \min_{\lambda} \quad & \log \left( \sum_{i=1}^{m_n} \exp \left( \sum_{n'=1}^{n-1} \sum_{j: s_j^{n'} \in s_i^n} \lambda_a^{n'} I(s_j^{n'} \in \mathcal{V}_{n'}) \right. \right. \\ & \left. \left. + \lambda_b^{n'} I(s_j^{n'} \in \mathcal{U}_{n'}) \right) \right) - \sum_{n'=1}^{n-1} \lambda_a^{n'} g_{n'} + \lambda_b^{n'} h_{n'}, \end{aligned}$$

where  $g_{n'} = \sum_{s_j^{n'} \in \mathcal{V}_{n'}} \hat{p}(s_j^{n'})$  and  $h_{n'} = \sum_{s_j^{n'} \in \mathcal{U}_{n'}} \hat{p}(s_j^{n'})$ .

Furthermore, let  $q_a^{n'}$  be the probability to observe a high frequency  $n'$ -gram appearing in any  $n$ -gram, and  $q_b^{n'}$  be the probability to observe a low frequency  $n'$ -gram appearing in any  $n$ -gram, we have

$$\begin{aligned} & \sum_{i=1}^{m_n} \exp \left( \sum_{n'=1}^{n-1} \sum_{j: s_j^{n'} \in s_i^n} \lambda_a^{n'} I(s_j^{n'} \in \mathcal{V}_{n'}) + \lambda_b^{n'} I(s_j^{n'} \in \mathcal{U}_{n'}) \right) \\ &= m_n \prod_{n'=1}^{n-1} (1 + q_a^{n'} \exp(\lambda_a^{n'}))(1 + q_b^{n'} \exp(\lambda_b^{n'})) + \mathcal{O}(\sqrt{m_n}). \end{aligned}$$

By skipping the term  $\mathcal{O}(\sqrt{m_n})$ , we further simplify the optimization problem as

$$\begin{aligned} \min_{\lambda} \quad & \sum_{n'=1}^{n-1} \log (1 + q_a^{n'} \exp(\lambda_a^{n'})) - \lambda_a^{n'} g_{n'} \\ & + \sum_{n'=1}^{n-1} \log (1 + q_b^{n'} \exp(\lambda_b^{n'})) - \lambda_b^{n'} h_{n'}, \end{aligned}$$

which is equivalent to

$$\begin{aligned} \lambda_a^{n'} &= \min_{\lambda} \log (1 + q_a^{n'} \exp(\lambda)) - \lambda g_{n'} \\ \lambda_b^{n'} &= \min_{\lambda} \log (1 + q_b^{n'} \exp(\lambda)) - \lambda h_{n'}. \end{aligned}$$

As illustrated by the above analysis, dual variables  $\lambda_a^{n'}$  and  $\lambda_b^{n'}$  will only depend on statistics  $q_a^{n'}$ ,  $q_b^{n'}$ ,  $g_{n'}$  and  $h_{n'}$ . They are independent from the detailed statistics  $\hat{p}(s_j^{n'})$  and how each  $n'$ -gram appears in different  $n$ -gram. Thus, this simple analysis does indicate, to some degree, that the solution obtained from the maximum entropy model can be universal, as long as  $n$ -grams follow skewed distributions like power law.

We informally demonstrate that transformer models utilize attention mechanisms to perform a sophisticated form of  $n$ -gram estimation, and the generation rule for such  $n$ -gram distributions could be universal. This is how universality is achieved in our proposed cross-domain knowledge transfer. However, we currently lack a concrete metric to evaluate the performance of knowledge transfer between different domains, which requires further investigation. Nonetheless, in our experimental study, we demonstrate that a transformer model (beit) (Bao et al., 2022) trained on images can perform well on cross-domain time series forecasting tasks.

## 5.2. Functionality

Our second question is: how does a pretrained LM benefit few-shot TS forecasting tasks? In this section, we aim to provide theoretical analysis to explore the potential advantages of using a pretrained LM for such tasks. All the proofs are provided in Appendix D.

In our numerical experiments, we obtain two interesting observations. First, the token similarity within a sample is

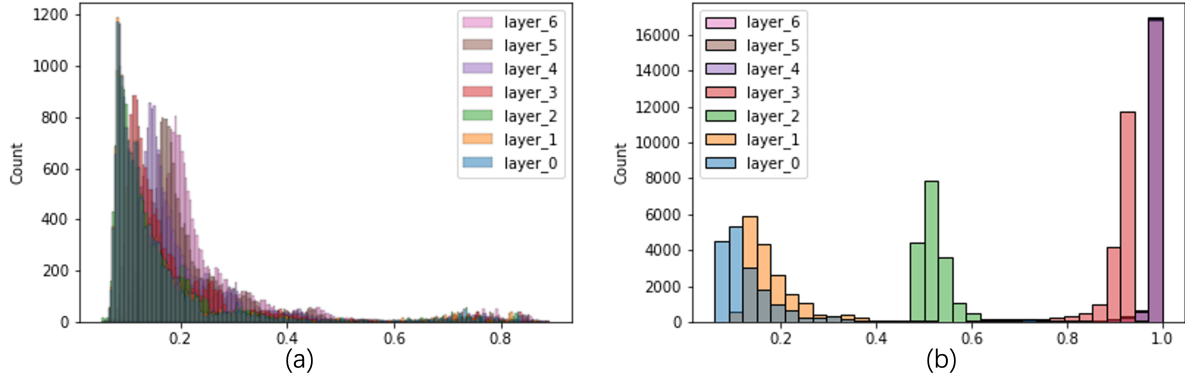


Figure 2. The token similarity within samples with respect to each layer (a):GPT-noPretrain-model, (b):GPT-Pretrained-model

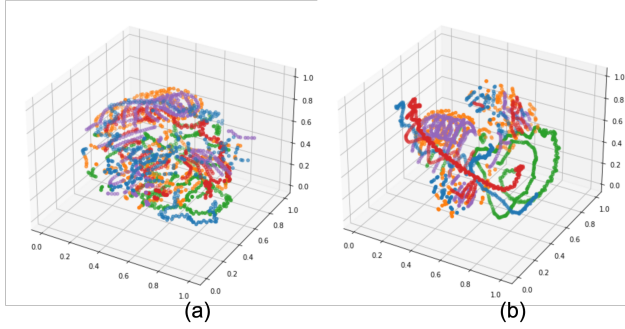


Figure 3. The t-SNE(van der Maaten & Hinton, 2008) visualization of sample feature maps for (a):GPT-FPT, (b):End2End-PatchTST-model

larger in pretrained LM. We report the layer-wise average token cosine similarity in ETTh2 experiment in Figure 2. In particular, Figure 2 (a) shows that in a fine-tuned random initialed GPT2 (6 Layer) model, the token similarity is around 0.1-0.2 among different layers. When switching to the frozen pretrained GPT2-FPT model, the token similarity significantly increases in the deep layers and eventually reaches more than 0.9 in the last layer. The ETTh2 dataset contains high volatility hourly information related to the electricity transformer temperature. In this situation, higher token similarity implies the high-frequency noise in the data is eased and only low-frequency information will be reserved. In another word, after going through the pretrained GPT2-FPT model, the signal-noise ratio is enhanced. We use the following theorem to characterize this behavior.

**Theorem 5.1** (informal). *We consider the self-attention for  $l$ -th query token. Let’s assume the input token  $x_i$  are bounded with mean  $\mu$  for  $i = 1, 2, \dots, n$ . Under mild conditions, with high probability, the output value token  $V_l$  converges to  $\mu W_v$  on the order of  $\mathcal{O}(n^{-1/2})$ , where  $W_v$  is*

*the parameter matrix to compute the value token.*

The Theorem 5.1 describes the self-attention structure can efficiently make output value token  $V_l$  converge its mean value  $\mu W_v$ . In the time series forecasting task, each token represents several adjacent points in a time series. When the time series has some periodical or translation invariant structures, by comparing a given token with other tokens, one could have a higher chance to figure out those invariant structures. This phenomenon is especially important in few-shot forecasting tasks. Without enough token noise distillation ability, the model will more likely tend to overfit due to insufficient training data.

The second observation is that for the pretrained GPT2-FPT model, the last transformer layer’s outputs, i.e., feature maps, are spread widely throughout the feature space. We report the t-SNE visualization of the feature maps for GPT2-FPT and an end2end model PatchTST in Figure 3. In Figure 3 (a) and (b), we color the samples chunked from the one single time series into the same color and the same configuration of the T-SNE is applied. One may observe that the feature maps of GPT2-FPT has less concentration compared to PatchTST. It implies the GPT2-FPT’s feature maps corresponding to different samples are more distinctive which eventually facilitates the learning ability of the last MLP layer. We use the following theorem to justify it.

**Theorem 5.2** (informal). *Let  $g_i$  and  $y_i$  be the feature map vector and forecasting targets for the sample  $i = 1, 2, \dots, N$  respectively, and we assume  $\frac{1}{N} \sum_{i=1}^N g_i g_i^\top \succeq \sigma I$  for some  $\sigma > 0$ . Under mild conditions, if we train an MLP layer that maps feature maps to forecasting targets via the stochastic gradient descent, the total step to reach some optimization tolerance is on the order of  $\mathcal{O}(\sigma^{-1})$ .*

The Theorem 5.2 considers the covariate matrix of feature maps being positive definite that indicates the set of all feature maps  $\{g_i\}$  spans the whole feature spaces, and the

higher spread level gives a larger  $\sigma$ . In this case, if we only want to learn an MLP layer, the problem reduces to a well-conditioned least-squared regression problem. Then the fast convergence rate is achieved.

Efficiently learning the last MLP layer plays a very important role in time series forecasting and can substantially impact the prediction performance. In Zeng et al. (2023), the authors show that learning a single MLP layer can also bring very promising performance. In few-shot forecasting, the pretrained GPT2 model may still preserve a highly diverse feature maps than end2end type models and eventually leads to fast learning speed on the last MLP layer.

Another possible benefit of wide spared feature maps is enhancing the model memorization ability when using a multi-layer decoder structure. In the literature on network memorization ability (e.g., Vardi et al. (2021); Yun et al. (2020)), the deep learning model tends to have better memorization ability when feature maps are well separated. In forecasting tasks, capturing extreme or rare behavior is very important. The pretrained GPT gains more capacity in the decoder to correctly forecast uncommon time series.

## 6. Experiment Analysis and other key results

### 6.1. Experiment analysis of GPT2-FPT model

In this section, we conduct experiments to analyze whether the self-attention frozen pretrained model improves performance compared with overall finetuning and random initialization. Firstly, we compare GPT2-backbone (6 Layers) FPT with the same model without freezing (No Freeze) and random initial model (No Pretrain). For the end2end paradigm No Pretrain GPT2-backbone (6 Layers), we directly train all parameters of the model. We summarize the results in Table 3 and Table 4. Then we analyze the performance of various layers to clarify our selection of GPT2-backbone (6 Layers) FPT.

**Finetune More Parameters** Compared with fine-tuning all parameters, self-attention frozen pretrained model GPT2-backbone (6 Layers) FPT achieves better performance on most datasets and yields an overall **12.7%** relative MSE reduction on 5% data and **11.5%** relative MSE reduction on 10% data. It verifies that frozen pretrained attention layers are effective for time series forecasting.

**Parameters Initialization** Compared with the random initial model, self-attention frozen pretrained model GPT2-backbone (6 Layers) FPT achieves better performance on most datasets and yields an overall **21.2%** relative MSE reduction on 5% data and **14.3%** relative MSE reduction on 10% data. It again suggests that a model pretrained on cross-domain data can achieve significant performance improvement in time series forecasting.

Table 3. Model analysis results on 5% data. We use prediction length  $O \in \{96, 192, 336, 720\}$  for ILI and  $O \in \{24, 36, 48, 60\}$  for others. GPT2-FPT represents GPT2-backbone (6 Layers) frozen pretrained transformer model. No Freeze and No Pretrain respectively represent GPT2-backbone (6 Layers) without freeze or pretrain. A lower MSE indicates better performance, and the best results are highlighted in bold. '-' means that 10% time series is not sufficient to constitute a training set.

Methods		GPT2-FPT		No Freeze		No Pretrain	
Metric		MSE	MAE	MSE	MAE	MSE	MAE
Weather	96	<b>0.175</b>	0.230	0.183	<b>0.229</b>	0.199	0.254
	192	<b>0.227</b>	<b>0.276</b>	0.275	0.300	0.262	0.302
	336	<b>0.286</b>	<b>0.322</b>	0.297	0.331	0.326	0.345
	720	<b>0.366</b>	<b>0.379</b>	0.380	0.388	0.405	0.396
ETTh1	96	<b>0.543</b>	<b>0.506</b>	0.671	0.564	0.882	0.643
	192	<b>0.748</b>	<b>0.580</b>	0.907	0.632	1.389	0.817
	336	<b>0.754</b>	<b>0.595</b>	0.931	0.655	2.968	1.149
	720	-	-	-	-	-	-
ETTh2	96	<b>0.376</b>	<b>0.421</b>	0.440	0.449	0.465	0.457
	192	<b>0.418</b>	<b>0.441</b>	0.503	0.478	0.614	0.536
	336	<b>0.408</b>	<b>0.439</b>	0.691	0.572	0.596	0.529
	720	-	-	-	-	-	-
ETTm1	96	<b>0.386</b>	<b>0.405</b>	0.429	0.432	0.394	0.410
	192	0.440	0.438	0.496	0.470	<b>0.432</b>	<b>0.432</b>
	336	<b>0.485</b>	<b>0.459</b>	0.535	0.489	0.491	0.464
	720	<b>0.557</b>	<b>0.499</b>	0.786	0.592	0.564	0.503
ETTm2	96	<b>0.199</b>	<b>0.280</b>	0.217	0.293	0.301	0.353
	192	<b>0.256</b>	<b>0.316</b>	0.300	0.350	0.321	0.365
	336	<b>0.318</b>	<b>0.353</b>	0.331	0.368	0.371	0.398
	720	<b>0.460</b>	0.439	<b>0.460</b>	<b>0.436</b>	0.659	0.528
ILI	24	4.225	1.588	<b>4.188</b>	<b>1.575</b>	4.861	1.624
	36	-	-	-	-	-	-
	48	-	-	-	-	-	-
	60	-	-	-	-	-	-

Table 4. No Pretrain and No Freeze results on 10% data. We use prediction length  $O \in \{96, 192, 336, 720\}$  for ILI and  $O \in \{24, 36, 48, 60\}$  for others.

Methods		GPT2-FPT		No Freeze		No Pretrain	
Metric		MSE	MAE	MSE	MAE	MSE	MAE
Weather	96	<b>0.163</b>	<b>0.215</b>	0.168	0.221	0.175	0.229
	192	<b>0.210</b>	<b>0.254</b>	0.238	0.286	0.244	0.287
	336	<b>0.256</b>	<b>0.292</b>	0.289	0.318	0.301	0.325
	720	<b>0.321</b>	<b>0.339</b>	0.398	0.383	0.390	0.378
ETTh1	96	<b>0.458</b>	<b>0.456</b>	0.605	0.532	0.680	0.560
	192	<b>0.570</b>	<b>0.516</b>	0.713	0.579	0.738	0.602
	336	<b>0.608</b>	<b>0.535</b>	0.747	0.586	0.893	0.641
	720	<b>0.725</b>	<b>0.591</b>	0.945	0.688	2.994	1.169
ETTh2	96	<b>0.331</b>	<b>0.374</b>	0.369	0.394	0.422	0.433
	192	<b>0.402</b>	<b>0.411</b>	0.464	0.455	0.482	0.466
	336	<b>0.406</b>	<b>0.433</b>	0.420	0.439	0.540	0.496
	720	<b>0.449</b>	<b>0.464</b>	0.535	0.515	0.564	0.519
ETTm1	96	0.390	0.404	0.429	0.430	<b>0.385</b>	<b>0.401</b>
	192	0.429	0.423	0.463	0.446	<b>0.426</b>	<b>0.421</b>
	336	<b>0.469</b>	<b>0.439</b>	0.510	0.470	0.506	0.455
	720	<b>0.569</b>	<b>0.498</b>	0.780	0.591	0.576	0.505
ETTm2	96	<b>0.188</b>	<b>0.269</b>	0.243	0.311	0.244	0.315
	192	<b>0.251</b>	<b>0.309</b>	0.307	0.352	0.318	0.363
	336	<b>0.307</b>	<b>0.346</b>	0.337	0.364	0.409	0.412
	720	<b>0.426</b>	<b>0.417</b>	0.471	0.440	0.473	0.450
ILI	24	<b>3.022</b>	<b>1.247</b>	3.231	1.266	3.375	1.281
	36	3.854	1.453	3.761	1.401	<b>3.056</b>	<b>1.277</b>
	48	4.603	1.571	4.539	1.556	<b>3.431</b>	<b>1.366</b>
	60	-	-	-	-	-	-

**The Number of GPT2 Layers** For most transformer-based



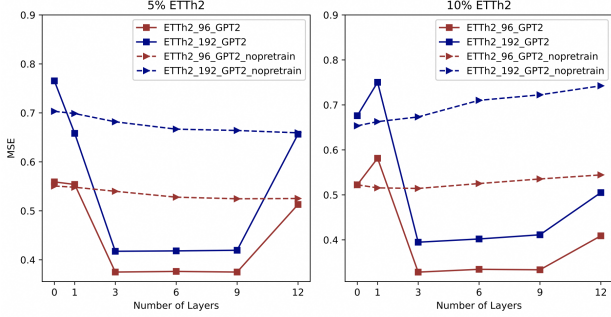


Figure 4. Comparison of pretrained and non-pretrained GPT2 with various layers on ETTh2. Color represents various prediction length  $O \in \{96, 192\}$  and line style means different models.

methods in time-series forecasting (Zhou et al., 2022; Wu et al., 2021; Nie et al., 2022), no more than 3 encoder layers are included. However, most pretrained models with at least 12 layers may suffer from overfitting in time series forecasting. To better balance performance and computational efficiency, we test using various numbers of layers on ETTh2. Additionally, we train a completely random initialized non-pretrained GPT2 as a comparison. The results are shown in Figure 4, for both 5% and 10% data, the pretrained model is unable to do well with few layers but significantly outperforms non-pretrained GPT2 with more attention blocks transferred from NLP. It indicates that pretrained attention layers produce a great benefit in time series forecasting. Also, the pretrained model achieves better performance between 3 and 9 layers. Thus GPT2 with 6 layers is chosen as our default architecture.

## 6.2. Ablation Study

In this section, we conduct ablation experiments to study which parameters are important to finetune. Since the input embedding and output layers are randomly initialized for adapting to a new domain, they must be trained. Then, we study adding layer normalization and positional embeddings to the list of finetuned parameters. Table 5 shows the results that re-train parameters of layer normalization and positional embeddings can bring certain benefits, especially in longer prediction lengths. Thus, we follow the standard practice to re-train positional embeddings and layer normalization.

## 6.3. Full Data Regular Time-series Forecasting

Here we investigate whether our architecture performs consistently well with more training data. Thus, we follow the classical experiment settings of (Nie et al., 2022) and conduct experiments on full data. For baselines, we cite their results from (Nie et al., 2022). The results are shown in Table 6. Overall, GPT2-backbone (6 Layers) FPT achieves

Table 5. Ablation by fixing positional embeddings or layer normalization on 5% ETTm1 and ETTm2. Parameters of GPT2-backbone(6 Layers) are successively added to the list of finetuned parameters.

Methods		Input & Output		+ LN		+ POS	
Metric		MSE	MAE	MSE	MAE	MSE	MAE
ETTm1	96	0.395	0.410	0.392	0.409	0.386	0.405
	192	0.444	0.438	0.436	0.435	0.440	0.438
	336	0.510	0.472	0.495	0.467	0.485	0.459
	720	0.607	0.517	0.564	0.503	0.557	0.499
ETTm2	96	0.198	0.282	0.198	0.279	0.199	0.280
	192	0.261	0.324	0.263	0.325	0.256	0.316
	336	0.336	0.377	0.322	0.356	0.318	0.353
	720	0.473	0.444	0.457	0.435	0.460	0.436

comparable performance to PatchTST, Dlinear and outperforms other baselines by a large margin. Compared with the second best transformer-based baseline method FEDformer, GPT2-backbone (6 Layers) FPT yields an overall **18.7%** relatively MSE reduction. It verifies the effectiveness of NLP pretrained model in time series forecasting, not limited to the few-shot setting.

## 6.4. Analysis of Data Volume

Results from Section 4.1 show that GPT2-backbone (6 Layers) FPT shows SOTA performance in few-shot learning tasks in which the model is trained on 5% data and 10% data. Plus, it has comparable performance with the SOTA baselines PatchTST and Dlinear on full sample forecasting setting as well. This phenomenon raises a question that how performance changes with an increase in data sample size. Thus, we conduct experiments on various percentages  $P \in \{5\%, 10\%, 20\%, 50\%, 80\%, 100\%\}$  of ETTh2. Figure 5 shows that the performance improvement for GPT2-backbone (6 Layers) FPT is almost flattened. These results illustrate that such a cross-domain FPT model is extremely efficient in few-shot time series forecasting and only requires a few fine-tuning samples to reach a SOTA performance. For more complete data, end2end training models start to catch up, but still, a GPT2-backbone (6 Layers) FPT model can be comparable to those SOTA end2end training algorithms.

## 6.5. Zero-shot Transfer Learning

We investigate the representation ability of GPT-backbone (6 Layers) FPT in zero-shot transfer learning tasks and follow the experiments settings of meta-learning based N-BEATS (Oreshkin et al., 2021). We conduct experiments on several univariate datasets, including M4 (Makridakis et al., 2020), M3 (Makridakis & Hibon, 2000), Tourism (Athanasopoulos et al., 2011), Electricity (Asuncion & Newman, 2007). All these datasets are obtained from (Godaheva et al., 2021).

Table 6. Results on full data. We use prediction length  $O \in \{96, 192, 336, 720\}$  for ILI and  $O \in \{24, 36, 48, 60\}$  for others. GPT2(6) and GPT2(0) represent GPT2-backbond 6 layers model and 0 layer model respectively. A lower MSE indicates better performance. **Black**: best, **Red**: second best.

Methods		GPT2(6)		GPT2(0)		DLinear		PatchTST		FEDformer		Autoformer		Informer	
Metric		MSE	MAE	MSE	MAE	MSE	MAE	MSE	MAE	MSE	MAE	MSE	MAE	MSE	MAE
Weather	96	<b>0.162</b>	<b>0.212</b>	0.181	0.232	0.176	0.237	<b>0.149</b>	<b>0.198</b>	0.217	0.296	0.266	0.336	0.300	0.384
	192	<b>0.204</b>	<b>0.248</b>	0.222	0.266	0.220	0.282	<b>0.194</b>	<b>0.241</b>	0.276	0.336	0.307	0.367	0.598	0.434
	336	<b>0.254</b>	<b>0.286</b>	0.270	0.299	0.265	0.319	<b>0.245</b>	<b>0.282</b>	0.339	0.380	0.359	0.395	0.578	0.523
	720	<b>0.326</b>	<b>0.337</b>	0.338	0.345	0.333	0.362	<b>0.314</b>	<b>0.334</b>	0.403	0.428	0.419	0.428	1.059	0.741
ETTh1	96	0.376	<b>0.397</b>	0.422	0.428	<b>0.375</b>	<b>0.399</b>	<b>0.370</b>	<b>0.399</b>	0.376	0.419	0.449	0.459	0.865	0.713
	192	0.416	<b>0.418</b>	0.466	0.450	<b>0.405</b>	<b>0.416</b>	<b>0.413</b>	0.421	0.420	0.448	0.500	0.482	1.008	0.792
	336	0.442	<b>0.433</b>	0.488	0.464	<b>0.439</b>	0.443	<b>0.422</b>	<b>0.436</b>	0.459	0.465	0.521	0.496	1.107	0.809
	720	<b>0.477</b>	<b>0.456</b>	0.485	0.478	0.472	0.490	<b>0.447</b>	<b>0.466</b>	0.506	0.507	0.514	0.512	1.181	0.865
ETTh2	96	<b>0.285</b>	<b>0.342</b>	0.318	0.368	0.289	0.353	<b>0.274</b>	<b>0.336</b>	0.346	0.388	0.358	0.397	3.755	1.525
	192	<b>0.354</b>	<b>0.389</b>	0.383	0.407	0.383	0.418	<b>0.339</b>	<b>0.379</b>	0.429	0.439	0.456	0.452	5.602	1.931
	336	<b>0.373</b>	<b>0.407</b>	0.406	0.427	0.448	0.443	<b>0.329</b>	<b>0.380</b>	0.496	0.487	0.482	0.486	4.721	1.835
	720	<b>0.406</b>	<b>0.441</b>	0.420	0.446	0.605	0.551	<b>0.379</b>	<b>0.422</b>	0.463	0.474	0.515	0.511	3.647	1.625
ETTm1	96	<b>0.292</b>	0.346	0.330	0.372	0.299	<b>0.343</b>	<b>0.290</b>	<b>0.342</b>	0.379	0.419	0.505	0.475	0.672	0.571
	192	<b>0.332</b>	0.372	0.371	0.394	0.335	<b>0.365</b>	<b>0.332</b>	<b>0.369</b>	0.426	0.441	0.553	0.496	0.795	0.669
	336	<b>0.366</b>	0.394	0.398	0.409	0.369	<b>0.386</b>	<b>0.366</b>	<b>0.392</b>	0.445	0.459	0.621	0.537	1.212	0.871
	720	<b>0.417</b>	<b>0.421</b>	0.454	0.440	0.425	<b>0.421</b>	<b>0.416</b>	<b>0.420</b>	0.543	0.490	0.671	0.561	1.166	0.823
ETTm2	96	<b>0.173</b>	<b>0.262</b>	0.192	0.281	0.167	0.269	<b>0.165</b>	<b>0.255</b>	0.203	0.287	0.255	0.336	0.365	0.453
	192	<b>0.229</b>	<b>0.301</b>	0.245	0.317	0.224	0.303	<b>0.220</b>	<b>0.292</b>	0.269	0.328	0.281	0.340	0.533	0.563
	336	<b>0.286</b>	<b>0.341</b>	0.302	0.352	0.281	0.342	<b>0.274</b>	<b>0.329</b>	0.325	0.366	0.339	0.372	1.363	0.877
	720	<b>0.378</b>	<b>0.401</b>	0.399	0.408	0.397	0.421	<b>0.362</b>	<b>0.385</b>	0.421	0.415	0.433	0.432	3.379	1.338
ILI	24	<b>2.063</b>	<b>0.881</b>	2.723	1.099	2.215	1.081	<b>1.319</b>	<b>0.754</b>	3.228	1.260	3.483	1.287	5.764	1.677
	36	<b>1.868</b>	<b>0.892</b>	2.027	0.966	1.963	0.963	<b>1.430</b>	<b>0.834</b>	2.679	1.080	3.103	1.148	4.755	1.467
	48	<b>1.790</b>	<b>0.884</b>	2.206	1.022	2.130	1.024	<b>1.553</b>	<b>0.815</b>	2.622	1.078	2.669	1.085	4.763	1.469
	60	1.979	<b>0.957</b>	<b>1.976</b>	0.983	2.368	1.096	<b>1.470</b>	<b>0.788</b>	2.857	1.157	2.770	1.125	5.264	1.564
ECL	96	0.139	0.238	<b>0.138</b>	0.234	0.140	0.237	<b>0.129</b>	<b>0.222</b>	0.186	0.302	0.196	0.313	0.304	0.393
	192	<b>0.153</b>	0.251	<b>0.152</b>	0.247	<b>0.153</b>	0.249	0.157	<b>0.240</b>	0.197	0.311	0.211	0.324	0.327	0.417
	336	0.169	0.266	<b>0.168</b>	0.263	0.169	0.267	<b>0.163</b>	<b>0.259</b>	0.213	0.328	0.214	0.327	0.333	0.422
	720	0.206	0.297	0.207	0.295	<b>0.203</b>	0.301	<b>0.197</b>	<b>0.290</b>	0.233	0.344	0.236	0.342	0.351	0.427
Traffic	96	<b>0.388</b>	0.282	0.390	<b>0.272</b>	0.410	0.282	<b>0.360</b>	<b>0.249</b>	0.576	0.359	0.597	0.371	0.733	0.410
	192	0.407	0.290	<b>0.403</b>	<b>0.276</b>	0.423	0.287	<b>0.379</b>	<b>0.256</b>	0.610	0.380	0.607	0.382	0.777	0.435
	336	<b>0.412</b>	0.294	0.413	<b>0.280</b>	0.436	0.296	<b>0.392</b>	<b>0.264</b>	0.608	0.375	0.623	0.387	0.776	0.434
	720	0.450	0.312	<b>0.447</b>	<b>0.298</b>	0.466	0.315	<b>0.432</b>	<b>0.286</b>	0.621	0.375	0.639	0.395	0.827	0.466

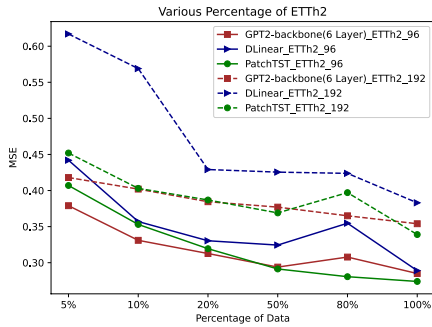


Figure 5. Results on various percentages of ETTh2. We choose percentages  $P \in \{5\%, 10\%, 20\%, 50\%, 80\%, 100\%\}$ . Line color represents different models and line style means various prediction lengths  $O \in \{96, 192\}$ .

**Task Definition** Each experiment contains two distinct datasets, source, and target datasets. The source dataset is used to train the model and then forecasts without fine-tuning in the target dataset. The target dataset is split into non-overlapping historical and test sequences. We use the

Table 7. Zero-shot transfer learning results. Dataset-specific metric aggregated over each dataset. A lower value indicates better performance. GPT2-FPT represents GPT2-backbone (6 Layers). The methods are named with format A-B (A is an algorithm, and B is the source dataset). **Black**: best, **Red**: second best, **Violet**: third best.

Methods	M4	M3	TOURISM	ELECTR
Metric	sMAPE	sMAPE	MAPE	ND
DeepAR-M4	-	14.76	24.79	0.532
N-BEATS-M4	-	<b>12.44</b>	<b>18.82</b>	<b>0.178</b>
N-BEATS-FR	<b>11.70</b>	<b>12.69</b>	<b>19.94</b>	0.205
DLinear-M4	-	14.03	28.51	<b>0.176</b>
DLinear-M3	<b>15.33</b>	-	28.45	-
GPT2-FPT-M4	-	<b>13.06</b>	<b>22.14</b>	<b>0.172</b>
GPT2-FPT-M3	<b>13.12</b>	-	24.99	-

historical sequence as input to the model, and the obtained output is used to calculate errors with the test sequences. Besides meta-learning-based models like N-BEATS, evaluated models' parameters are not allowed any adjustment using the forecasting phase. Also, same as (Oreshkin et al., 2021), each data set adopts a specific metric (M4: sMAPE;

Table 8. Results of frozen pretrained transformer variants on 5% ETTh2 and ETTm2. We use prediction length  $O \in \{96, 192, 336, 720\}$ . A lower MSE indicates better performance. **Black**: best, **Red**: second best, **Violet**: third best. '-' means that 5% time series is not sufficient to constitute a training set.

Methods	Metric	ETTh2				ETTM2			
		96	192	336	720	96	192	336	720
GPT2-backbone(6 Layers)	MSE	<b>0.376</b>	<b>0.421</b>	<b>0.408</b>	-	<b>0.199</b>	<b>0.256</b>	<b>0.318</b>	0.460
	MAE	<b>0.419</b>	<b>0.441</b>	<b>0.439</b>	-	<b>0.280</b>	<b>0.316</b>	<b>0.353</b>	<b>0.436</b>
BERT-backbone(6 Layers)	MSE	<b>0.397</b>	0.480	0.481	-	0.222	0.281	<b>0.331</b>	<b>0.441</b>
	MAE	<b>0.418</b>	0.465	<b>0.472</b>	-	0.300	0.335	<b>0.367</b>	<b>0.428</b>
BEiT-backbone(6 Layers)	MSE	0.405	<b>0.448</b>	0.524	-	<b>0.208</b>	<b>0.272</b>	<b>0.331</b>	<b>0.452</b>
	MAE	<b>0.418</b>	<b>0.446</b>	0.500	-	<b>0.291</b>	<b>0.326</b>	<b>0.362</b>	<b>0.433</b>
DLinear(Zeng et al., 2023)	MSE	0.442	0.617	1.424	-	0.236	0.306	0.380	0.674
	MAE	0.456	0.542	0.849	-	0.326	0.373	0.423	0.583
PatchTST(Nie et al., 2022)	MSE	0.401	<b>0.452</b>	<b>0.464</b>	-	<b>0.206</b>	<b>0.264</b>	<b>0.334</b>	<b>0.454</b>
	MAE	0.421	<b>0.455</b>	<b>0.469</b>	-	<b>0.288</b>	<b>0.324</b>	<b>0.367</b>	0.483
FEDformer(Zhou et al., 2022)	MSE	<b>0.390</b>	0.457	<b>0.477</b>	-	0.299	0.290	0.378	0.523
	MAE	0.424	0.465	0.483	-	0.320	0.361	0.427	0.510
Autoformer(Wu et al., 2021)	MSE	0.428	0.496	0.486	-	0.232	0.291	0.478	0.533
	MAE	0.468	0.504	0.496	-	0.322	0.357	0.517	0.538

M3: sMAPE; TOURISM: MAPE; ELECTR: ND)

**Key Results** Apart from N-BEATS and DeepAR (Salinas et al., 2020), we further evaluate DLinear (Zeng et al., 2023) in the zero-shot learning tasks. This task is used for evaluating the cross datasets adaption ability of our proposed algorithm. Traditionally, meta-learning-based algorithm like N-BEATS outperforms others by a large margin in such tasks. The results are summarized in Table 7. The GPT2-backbone(6 Layers) FPT model consistently outperform DLinear and deepAR. In particular, on some datasets, such as M4 and TOURISM, the improvement can be more than 15%. Also, the proposed method is comparable to N-BEATS without any meta-learning design and outperforms N-BEATS in the ELECTR dataset. We attribute this to the knowledge transfer capability from the FPT model. Detailed results are provided in Appendix C.3.

### 6.6. Knowledge transfer with other Pretrained Transformer Models

We investigate how other pretrained transformer models perform and whether other domains can also help. Another NLP pretrained model BERT (Devlin et al., 2019) and the CV pretrained model BEiT (Bao et al., 2022) are trained on 5% ETTh2 and 5% ETTm2. Similar to GPT2, we only reserve 6 layers and freeze attention blocks. Our results are shown in Table 8 that BERT-backbone (6 Layers) FPT and BEiT-backbone (6 Layers) FPT are comparable to PatchTST and remarkably surpass other baselines. We come to the conclusion that the universality of our proposed architecture holds across other pretrained-transformer models. Moreover, the domain of successful knowledge transfer in time series forecasting is not limited to natural language. Knowledge from the CV domain can also help, supported by BEiT’s experimental results.

## 7. Conclusions

In this paper, we have demonstrated that utilizing a pretrained language model can significantly enhance time series forecasting in few-shot learning, full data learning, and zero-shot learning scenarios. While transfer learning has been extensively studied in other domains, there has been limited work on transfer learning for time series data, primarily due to the complexity and diversity of such data across various domains. To the best of our knowledge, our work represents the first successful attempt to perform cross-domain knowledge transfer for time series forecasting, achieving state-of-the-art performance in various forecasting tasks. Our findings are supported by empirical and theoretical evidence. Moving forward, we aim to investigate more time series applications where cross-domain knowledge transfer can be beneficial, and further understand the underlying mechanism for cross-domain knowledge transfer in the context of time series data.

## References

- Asuncion, A. and Newman, D. Uci machine learning repository, 2007.
- Athanasopoulos, G., Hyndman, R. J., Song, H., and Wu, D. C. The tourism forecasting competition. *International Journal of Forecasting*, 27(3):822–844, 2011.
- Bao, H., Wang, W., Dong, L., Liu, Q., Mohammed, O. K., Aggarwal, K., Som, S., and Wei, F. Vlmo: Unified vision-language pre-training with mixture-of-modality-experts. *arXiv preprint arXiv:2111.02358*, 2021.
- Bao, H., Dong, L., Piao, S., and Wei, F. BEiT: BERT pre-training of image transformers. In *International Conference on Learning Representations*, 2022.
- Böse, J.-H., Flunkert, V., Gasthaus, J., Januschowski, T., Lange, D., Salinas, D., Schelter, S., Seeger, M., and Wang, Y. Probabilistic demand forecasting at scale. *Proceedings of the VLDB Endowment*, 10(12):1694–1705, 2017.
- Box, G. E. and Jenkins, G. M. Some recent advances in forecasting and control. *Journal of the Royal Statistical Society. Series C (Applied Statistics)*, 17(2):91–109, 1968.
- Box, G. E. and Pierce, D. A. Distribution of residual autocorrelations in autoregressive-integrated moving average time series models. *Journal of the American statistical Association*, 65(332):1509–1526, 1970.
- Chung, J., Gulcehre, C., Cho, K., and Bengio, Y. Empirical evaluation of gated recurrent neural networks on sequence modeling. *arXiv preprint arXiv:1412.3555*, 2014.

- Connor, J. T., Martin, R. D., and Atlas, L. E. Recurrent neural networks and robust time series prediction. *IEEE transactions on neural networks*, 5(2):240–254, 1994.
- Courty, P. and Li, H. Timing of seasonal sales. *The Journal of Business*, 72(4):545–572, 1999.
- Devlin, J., Chang, M., Lee, K., and Toutanova, K. BERT: pre-training of deep bidirectional transformers for language understanding. In *Proceedings of the 2019 Conference of the North American Chapter of the Association for Computational Linguistics: Human Language Technologies (NAACL-HLT)*, Minneapolis, MN, USA, June 2-7, 2019, pp. 4171–4186, 2019.
- Dosovitskiy, A., Beyer, L., Kolesnikov, A., Weissenborn, D., Zhai, X., Unterthiner, T., Dehghani, M., Minderer, M., Heigold, G., Gelly, S., Uszkoreit, J., and Houshy, N. An image is worth 16x16 words: Transformers for image recognition at scale. In *9th International Conference on Learning Representations (ICLR)*, Austria, May 3-7, 2021, 2021.
- Elhage, N., Nanda, N., Olsson, C., Henighan, T., Joseph, N., Mann, B., Askell, A., Bai, Y., Chen, A., Conerly, T., DasSarma, N., Drain, D., Ganguli, D., Hatfield-Dodds, Z., Hernandez, D., Jones, A., Kernion, J., Lovitt, L., Ndousse, K., Amodei, D., Brown, T., Clark, J., Kaplan, J., McCandlish, S., and Olah, C. A mathematical framework for transformer circuits. *Transformer Circuits Thread*, 2021. <https://transformer-circuits.pub/2021/framework/index.html>.
- Godahewa, R., Bergmeir, C., Webb, G. I., Hyndman, R. J., and Montero-Manso, P. Monash time series forecasting archive. In *Neural Information Processing Systems Track on Datasets and Benchmarks*, 2021.
- Gonzalez-Vidal, A., Jimenez, F., and Gomez-Skarmeta, A. F. A methodology for energy multivariate time series forecasting in smart buildings based on feature selection. *Energy and Buildings*, 196:71–82, 2019.
- Hewamalage, H., Bergmeir, C., and Bandara, K. Recurrent neural networks for time series forecasting: Current status and future directions. *International Journal of Forecasting*, 37(1):388–427, 2021.
- Hochreiter, S. and Schmidhuber, J. Long short-term memory. *Neural computation*, 9(8):1735–1780, 1997.
- Houshy, N., Giurgiu, A., Jastrzebski, S., Morrone, B., De Laroussilhe, Q., Gesmundo, A., Attariyan, M., and Gelly, S. Parameter-efficient transfer learning for nlp. In *International Conference on Machine Learning*, pp. 2790–2799. PMLR, 2019.
- Hyndman, R. and Athanasopoulos, G. *Forecasting: Principles and Practice*. OTexts, Australia, 3rd edition, 2021.
- Ismail Fawaz, H., Forestier, G., Weber, J., Idoumghar, L., and Muller, P.-A. Transfer learning for time series classification. In *IEEE International Conference on Big Data*, pp. 1367–1376, 2018.
- Kim, T., Kim, J., Tae, Y., Park, C., Choi, J.-H., and Choo, J. Reversible instance normalization for accurate time-series forecasting against distribution shift. In *International Conference on Learning Representations*, 2022.
- Lacoste-Julien, S., Schmidt, M., and Bach, F. A simpler approach to obtaining an  $\mathcal{O}(1/t)$  convergence rate for the projected stochastic subgradient method. *arXiv preprint arXiv:1212.2002*, 2012.
- Lim, B., Alaa, A., and van der Schaar, M. Forecasting treatment responses over time using recurrent marginal structural networks. *NeurIPS*, 18:7483–7493, 2018.
- Lu, K., Grover, A., Abbeel, P., and Mordatch, I. Frozen pretrained transformers as universal computation engines. *Proceedings of the AAAI Conference on Artificial Intelligence*, 36(7):7628–7636, Jun. 2022.
- Makridakis, S. and Hibon, M. The m3-competition: results, conclusions and implications. *International journal of forecasting*, 16(4):451–476, 2000.
- Makridakis, S., Spiliotis, E., and Assimakopoulos, V. The m4 competition: 100,000 time series and 61 forecasting methods. *International Journal of Forecasting*, 36(1): 54–74, 2020.
- Nie, Y., Nguyen, N. H., Sinthong, P., and Kalagnanam, J. A time series is worth 64 words: Long-term forecasting with transformers. *ArXiv*, abs/2211.14730, 2022.
- Olsson, C., Elhage, N., Nanda, N., Joseph, N., DasSarma, N., Henighan, T., Mann, B., Askell, A., Bai, Y., Chen, A., Conerly, T., Drain, D., Ganguli, D., Hatfield-Dodds, Z., Hernandez, D., Johnston, S., Jones, A., Kernion, J., Lovitt, L., Ndousse, K., Amodei, D., Brown, T., Clark, J., Kaplan, J., McCandlish, S., and Olah, C. In-context learning and induction heads. *Transformer Circuits Thread*, 2022. <https://transformer-circuits.pub/2022/in-context-learning-and-induction-heads/index.html>.
- Oreshkin, B. N., Carpo, D., Chapados, N., and Bengio, Y. Meta-learning framework with applications to zero-shot time-series forecasting. In *Proceedings of the AAAI Conference on Artificial Intelligence*, number 10, pp. 9242–9250, 2021.
- Radford, A. and Narasimhan, K. Improving language understanding by generative pre-training. 2018.



- Radford, A., Wu, J., Child, R., Luan, D., Amodei, D., and Sutskever, I. Language models are unsupervised multitask learners. 2019.
- Rao, Y., Zhao, W., Zhu, Z., Lu, J., and Zhou, J. Global filter networks for image classification. *Advances in Neural Information Processing Systems (NeurIPS)*, 34, 2021.
- Salinas, D., Flunkert, V., Gasthaus, J., and Januschowski, T. Deepar: Probabilistic forecasting with autoregressive recurrent networks. *International Journal of Forecasting*, 36(3):1181–1191, 2020.
- Touvron, H., Cord, M., Douze, M., Massa, F., Sablayrolles, A., and Jégou, H. Training data-efficient image transformers & distillation through attention. In *International Conference on Machine Learning*, pp. 10347–10357. PMLR, 2021.
- van der Maaten, L. and Hinton, G. E. Visualizing data using t-sne. *Journal of Machine Learning Research*, 9: 2579–2605, 2008.
- Vardi, G., Yehudai, G., and Shamir, O. On the optimal memorization power of relu neural networks. *arXiv preprint arXiv:2110.03187*, 2021.
- Vaswani, A., Shazeer, N., Parmar, N., Uszkoreit, J., Jones, L., Gomez, A. N., Kaiser Lukasz, and Polosukhin, I. Attention is all you need. *arXiv preprint arXiv:1706.03762*, 2017.
- Wang, P., Wang, X., Wang, F., Lin, M., Chang, S., Li, H., and Jin, R. Kvt: k-nn attention for boosting vision transformers. In *Computer Vision–ECCV 2022: 17th European Conference, Tel Aviv, Israel, October 23–27, 2022, Proceedings, Part XXIV*, pp. 285–302. Springer, 2022.
- Wen, Q., Zhou, T., Zhang, C., Chen, W., Ma, Z., Yan, J., and Sun, L. Transformers in time series: A survey. *arXiv preprint arXiv:2202.07125*, 2022.
- Wolf, T., Debut, L., Sanh, V., Chaumond, J., Delangue, C., Moi, A., Cistac, P., Rault, T., Louf, R., Funtowicz, M., Davison, J., Shleifer, S., von Platen, P., Ma, C., Jernite, Y., Plu, J., Xu, C., Scao, T. L., Gugger, S., Drame, M., Lhoest, Q., and Rush, A. M. Transformers: State-of-the-art natural language processing. In *Proceedings of the 2020 Conference on Empirical Methods in Natural Language Processing: System Demonstrations*, pp. 38–45, Online, October 2020. Association for Computational Linguistics. URL <https://www.aclweb.org/anthology/2020.emnlp-demos.6>.
- Wu, H., Xu, J., Wang, J., and Long, M. Autoformer: Decomposition transformers with auto-correlation for long-term series forecasting. In *Advances in Neural Information Processing Systems (NeurIPS)*, pp. 101–112, 2021.
- Yang, C.-H. H., Tsai, Y.-Y., and Chen, P.-Y. Voice2series: Reprogramming acoustic models for time series classification. In *International Conference on Machine Learning*, pp. 11808–11819, 2021.
- Yun, C., Chang, Y.-W., Bhojanapalli, S., Rawat, A. S., Reddi, S., and Kumar, S. O(n) connections are expressive enough: Universal approximability of sparse transformers. *Advances in Neural Information Processing Systems*, 33:13783–13794, 2020.
- Zeng, A., Chen, M., Zhang, L., and Xu, Q. Are transformers effective for time series forecasting? 2023.
- Zhang, C., Song, D., Chen, Y., Feng, X., Lumezanu, C., Cheng, W., Ni, J., Zong, B., Chen, H., and Chawla, N. V. A deep neural network for unsupervised anomaly detection and diagnosis in multivariate time series data. In *Proceedings of the AAAI Conference on Artificial Intelligence*, volume 33, pp. 1409–1416, 2019.
- Zhang, J. and Nawata, K. Multi-step prediction for influenza outbreak by an adjusted long short-term memory. *Epidemiology & Infection*, 146(7):809–816, 2018.
- Zhou, H., Zhang, S., Peng, J., Zhang, S., Li, J., Xiong, H., and Zhang, W. Informer: Beyond efficient transformer for long sequence time-series forecasting. In *Proceedings of AAAI*, 2021.
- Zhou, T., Ma, Z., Wen, Q., Wang, X., Sun, L., and Jin, R. FEDformer: Frequency enhanced decomposed transformer for long-term series forecasting. In *Proc. 39th International Conference on Machine Learning (ICML 2022)*, 2022.

## A. Related Works

**Time Series Forecasting** Time series forecasting models can be roughly divided into three categories, ranging from the classic ARIMA models to the most recent transformer models. The first generation of well-discussed models can be dated back to auto-regressive family, such as ARIMA (Box & Jenkins, 1968; Box & Pierce, 1970) that follows the Markov process and recursively execute sequential forecasting. However, it is limited to stationary sequences while most time series is non-stationary. Additionally, with the bloom of deep neural networks, recurrent neural networks (RNNs), such as LSTM (Hochreiter & Schmidhuber, 1997) and GRU (Chung et al., 2014), were designed for sequential tasks. Yet the recurrent model is not efficient for training and long-term dependencies are still under resolved.

Recently, transformer models have achieve great progress in NLP (Vaswani et al., 2017; Devlin et al., 2019; Radford et al., 2019) and CV (Dosovitskiy et al., 2021; Bao et al., 2022) tasks. Also, a large amount of transformer models are proposed to apply to time series forecasting (Wen et al., 2022). In the following, we briefly introduce several representative algorithms. Informer (Zhou et al., 2021) proposes a probability sparse attention mechanism to deal with long-term dependencies. Autoformer (Wu et al., 2021) introduces a decomposition transformer architecture and replaces the attention module with an Auto-Correlation mechanism. FEDformer (Zhou et al., 2022) uses Fourier enhanced structure to improve computational efficiency and achieves linear complexity. Similar to patching in ViT (Dosovitskiy et al., 2021), PatchTST (Nie et al., 2022) employs segmentation of time series that divide a sequence into patches to increase input length and reduce information redundancy. Besides, a simple MLP-based model DLinear (Zeng et al., 2023) outperforms most transformer models and it validates channel-independence works well in time series forecasting.

## B. Dataset Details

In this section, we separately summarize dataset details of few-shot learning and zero-shot learning. Datasets of full data forecasting are the same as few-shot learning.

**Datasets of Few-shot Learning** The details of few-shot learning datasets are shown as follows: 1) ETT datasets (Zhou et al., 2021) contains electricity load of various resolutions (ETTh & ETTm) from two electricity stations. 2) Weather contains 21 meteorological indicators of Germany within 1 year; 3) Illness contains the influenza-like illness patients in the United States. Table 9 summarizes details of feature statistics.

Table 9. Dataset details of few-shot learning.

Dataset	Length	Dimension	Frequency
ETTh	17420	8	1 hour
ETTM	69680	8	15 min
Weather	52696	22	10 min
ILI	966	8	7 days

**Datasets of Zero-shot Learning** The details of zero-shot learning datasets are shown as follows: 1) M4 is a large and divers dataset that contains time series of various frequencies, including business, financial and economic forecasting; 2) M3 is smaller than M4, but also contains time series from diverse domains and frequencies; 3) TOURISM is the dataset of tourism activities with different frequencies and contains a much higher fraction of erratic series compared with M4; 4) ELECTRA represents the electricity usage monitoring of 370 customers over three years. Table 7 summarizes details of the datasets and zero-shot mapping between source and target.

## C. Experimental Details

All the deep learning networks are implemented in PyTorch and trained on NVIDIA V100 32GB GPUs. We use the pretrained models from (Wolf et al., 2020) for experiments. For few-shot learning, an early stopping counter is employed to stop the training process after three epochs if no loss degradation on the valid set is observed. Plus, we convert the multivariate data into univariate data. Specifically, we treat each feature of the sequence as a single time series. This is mainly for memory efficiency after patching of GPT2-backbone (6 Layers) and previous works, DLinear and PatchTST, have proved the effectiveness of channel-independence.

Table 10. Datasets and mapping details of zero-shot learning.

	Dataset		Mapping	
	Length	Horizon	M4	M3
M3 Yearly	645	6	Yearly	-
M3 Quarterly	756	8	Quarterly	-
M3 Monthly	1428	18	Monthly	-
M3 Others	174	8	Monthly	-
M4 Yearly	23000	6	-	Yearly
M4 Quarterly	24000	8	-	Quarterly
M4 Monthly	48000	18	-	Monthly
M4 Weekly	359	13	-	Monthly
M4 Daily	4227	14	-	Monthly
M4 Hourly	414	48	-	Monthly
TOURISM Yearly	518	4	Yearly	Yearly
TOURISM Quarterly	427	8	Quarterly	Quarterly
TOURISM Monthly	366	24	Monthly	Monthly
ELECTR	1311	168	Hourly	Monthly

### C.1. Accuracy Metrics

For few-shot learning, we use mean square error (MSE) and mean absolute error (MAE) as metrics. For zero-shot learning, mean absolute percentage error (MAPE) is used for TOURISM; symmetric MAPE (sMAPE) is used for M3 and M4; normalized deviation (ND) is used for ELECTR. All experiments are repeated 3 times and the mean of the metrics is used in the final results.

### C.2. Detailed Results of Few-shot Learning

Table 11 lists both mean and STD for GPT2-backbone (6 Layers), DLinear and PatchTST with 3 runs on 5% ETTh2 and ETTm2. The results show a small variance in performance of GPT2-backbone (6 Layers) that represents the stability of GPT2-backbone (6 Layers).

Table 11. A subset of results showing both Mean and STD on 5% datasets.

Methods		GPT2-backbone(6 Layers)		DLinear		PatchTST	
Metric		MSE	MAE	MSE	MAE	MSE	MAE
ETTh2	96	0.376 $\pm$ 0.0072	0.421 $\pm$ 0.0054	0.442 $\pm$ 0.0089	0.456 $\pm$ 0.0071	0.401 $\pm$ 0.0044	0.421 $\pm$ 0.0031
	192	0.418 $\pm$ 0.0013	0.441 $\pm$ 0.0014	0.617 $\pm$ 0.0045	0.542 $\pm$ 0.0019	0.452 $\pm$ 0.0028	0.455 $\pm$ 0.0017
	336	0.408 $\pm$ 0.0006	0.439 $\pm$ 0.0002	1.426 $\pm$ 0.0442	0.849 $\pm$ 0.0175	0.464 $\pm$ 0.0018	0.469 $\pm$ 0.0011
	720	-	-	-	-	-	-
ETTM2	96	0.199 $\pm$ 0.0040	0.280 $\pm$ 0.0042	0.236 $\pm$ 0.0024	0.326 $\pm$ 0.0025	0.206 $\pm$ 0.0011	0.288 $\pm$ 0.0009
	192	0.256 $\pm$ 0.0030	0.316 $\pm$ 0.0017	0.306 $\pm$ 0.0049	0.373 $\pm$ 0.0047	0.264 $\pm$ 0.0013	0.324 $\pm$ 0.0011
	336	0.318 $\pm$ 0.0046	0.353 $\pm$ 0.0032	0.380 $\pm$ 0.0025	0.423 $\pm$ 0.0017	0.334 $\pm$ 0.0029	0.367 $\pm$ 0.0017
	720	0.460 $\pm$ 0.0132	0.436 $\pm$ 0.0066	0.674 $\pm$ 0.0005	0.583 $\pm$ 0.0003	0.454 $\pm$ 0.0030	0.432 $\pm$ 0.0015

### C.3. Detailed Results of Zero-shot Learning

Here, we list detailed performance of zero-shot learning. For each dataset, we separately list the performance of models under diverse frequency. Compared to the most recent published method DLinear, GPT2-backbone (6 Layers) performs superior in most situations. Also, GPT2-backbone (6 Layers) does not use any information of the test data, but achieve comparable performance of meta-learning based N-BEATS.

Table 12. Zero-shot performance on M4 (sMAPE). GPT2-FPT represents GPT2-backbone (6 Layers).

	Yearly (23k)	Quarterly (24k)	Monthly (48k)	Others (5k)	Average (100k)
N-BEATS-FR	13.267	9.596	12.676	4.696	11.675
DLinear-M3	14.193	18.856	14.765	9.194	15.337
GPT-FPT-M3	13.740	10.787	14.630	7.081	13.125

Table 13. Zero-shot performance on M3 (sMAPE). GPT2-FPT represents GPT2-backbone (6 Layers).

	Yearly (645)	Quarterly (756)	Monthly (1428)	Others (174)	Average (3003)
DeepAR-M4	14.76	9.28	16.15	13.09	14.76
N-BEATS-M4	15.07	9.07	13.19	4.29	12.38
N-BEATS-FR	16.43	9.05	13.30	4.51	12.61
DLinear-M4	17.43	9.74	15.65	6.81	14.03
GPT2-FPT-M4	16.42	10.13	14.10	4.81	13.06

Table 14. Zero-shot performance on Tourism (MAPE). GPT2-FPT represents GPT2-backbone (6 Layers).

	Yearly (518)	Quarterly (427)	Monthly (366)	Average (1311)
DeepAR-M4	21.51	22.01	26.64	24.79
N-BEATS-M4	23.57	14.66	19.32	18.82
N-BEATS-FR	23.43	14.45	20.47	19.46
DLinear-M4	39.59	18.30	24.76	28.51
DLinear-M3	38.20	17.21	27.76	28.45
GPT2-FPT-M4	27.17	16.21	21.92	22.14
GPT2-FPT-M3	27.46	17.66	30.03	24.99

## D. Proof

### D.1. Theorem 5.1

We denote  $x_i$  as  $i$ -th element of vector  $\mathbf{x}$ ,  $\mathbf{W}_{ij}$  as the element at  $i$ -th row and  $j$ -th column of matrix  $\mathbf{W}$ , and  $\mathbf{W}_j$  as the  $j$ -th row of matrix  $\mathbf{W}$ . Moreover, we denote  $\mathbf{x}_i$  as the  $i$ -th patch (token) of the inputs with  $\mathbf{x}_i = \mathbf{X}_i$ .

Before given the formal statement of the Theorem 5.1, we first show the assumptions.

1. The token  $\mathbf{x}_i$  is the sub-gaussian random vector with mean  $\boldsymbol{\mu}_i$  and variance  $(\sigma^2/d)I$  for  $i = 1, 2, \dots, n$ .
2.  $\boldsymbol{\mu}$  follows a discrete distribution with finite values  $\boldsymbol{\mu} \in \mathcal{V}$ . Moreover, there exist  $0 < \nu_1, 0 < \nu_2 < \nu_4$  such that a)  $\|\boldsymbol{\mu}_i\| = \nu_1$ , and b)  $\boldsymbol{\mu}_i \mathbf{W}_Q \mathbf{W}_K^T \boldsymbol{\mu}_i \in [\nu_2, \nu_4]$  for all  $i$  and  $|\boldsymbol{\mu}_i \mathbf{W}_Q \mathbf{W}_K^T \boldsymbol{\mu}_j^T| \leq \nu_2$  for all  $\boldsymbol{\mu}_i \neq \boldsymbol{\mu}_j \in \mathcal{V}$ .
3.  $\mathbf{W}_V$  and  $\mathbf{W}_Q \mathbf{W}_K^T$  are element-wise bounded with  $\nu_5$  and  $\nu_6$  respectively, that is,  $|\mathbf{W}_V^{(ij)}| \leq \nu_5$  and  $|\mathbf{W}_Q \mathbf{W}_K^T|^{(ij)}| \leq \nu_6$ , for all  $i, j$  from 1 to  $d$ .

In above assumptions we ensure that for a given query patch, the difference between the clustering center and noises are large enough to be distinguished.

**Theorem D.1** (formal statement of Theorem 5.1). *Let patch  $\mathbf{x}_i$  be  $\sigma^2$ -subgaussian random variable with mean  $\boldsymbol{\mu}_i$  and all  $n$  patches follows the same clustering center of query  $l$ . Per Assumptions aforementioned, when  $\sqrt{d} \geq 3(\psi(\delta, d) + \nu_2 + \nu_4)$ , then with probability  $1 - 5\delta$ , we have*



$$\left\| \frac{\sum_{i=1}^n \exp\left(\frac{1}{\sqrt{d}} \mathbf{x}_i \mathbf{W}_Q \mathbf{W}_K^\top \mathbf{x}_i\right) \mathbf{x}_i \mathbf{W}_V}{\sum_{j=1}^n \exp\left(\frac{1}{\sqrt{d}} \mathbf{x}_j \mathbf{W}_Q \mathbf{W}_K^\top \mathbf{x}_j\right)} - \boldsymbol{\mu}_l \mathbf{W}_V \right\|_\infty \leq 4 \exp\left(\frac{\psi(\delta, d)}{\sqrt{d}}\right) \sigma \nu_5 \sqrt{\frac{2}{dn} \log\left(\frac{2d}{\delta}\right)} + 7 \left[ \exp\left(\frac{\nu_2 - \nu_4 + \psi(\delta, d)}{\sqrt{d}}\right) - 1 \right] \|\boldsymbol{\mu}_l \mathbf{W}_V\|_\infty,$$

where  $\psi(\delta, d) = 2\sigma\nu_1\nu_6\sqrt{2\log\left(\frac{1}{\delta}\right)} + 2\sigma^2\nu_6\log\left(\frac{d}{\delta}\right)$ .

*Proof.* See the proof of Lemma 2 in Wang et al. (2022) with  $k_1 = k = n$ .  $\square$

## D.2. Theorem 5.2

We first give the formal statement of Theorem 5.2.

**Theorem D.2** (formal statement of Theorem 5.2). *Let  $\mathbf{g}_i \in \mathbb{R}^d$  and  $\mathbf{y}_i \in \mathbb{R}^T$  be the feature map vector and forecasting targets for the sample  $i = 1, 2, \dots, N$  respectively, and we assume  $\frac{1}{N} \sum_{i=1}^N \mathbf{g}_i \mathbf{g}_i^\top \succeq \sigma I$  for some  $\sigma > 0$ . We want to learn a matrix  $\mathbf{W} \in \mathbb{R}^{d \times T}$  from the following optimization problem:*

$$\mathbf{W} = \arg \min \frac{1}{2N} \sum_{i=1}^N \|\mathbf{W} \mathbf{g}_i - \mathbf{y}_i\|_2^2. \quad (1)$$

If we apply stochastic gradient descent with diminishing step sizes  $\eta_t = \frac{1}{\sigma t}$  at step  $t$ , we will need  $t = \tilde{\mathcal{O}}(\epsilon^{-1} \sigma^{-1})$  steps to reach

$$\frac{1}{t} \sum_{j=1}^t \left( \frac{1}{2N} \sum_{i=1}^N \|\mathbf{W}_j \mathbf{g}_i - \mathbf{y}_i\|_2^2 \right) - \frac{1}{2N} \sum_{i=1}^N \|\mathbf{W}^* \mathbf{g}_i - \mathbf{y}_i\|_2^2 \leq \epsilon, \quad (2)$$

where  $\mathbf{W}^*$  is the optimal solution and  $\mathbf{W}_j$  is the  $j$  step's solution and  $\tilde{\mathcal{O}}$  we suppress the logarithmic dependence.

*Proof.* As we assume  $\frac{1}{N} \sum_{i=1}^T \mathbf{g}_i \mathbf{g}_i^\top \succeq \sigma I$ , the hessian of optimization problem in (1) is also positive definite, which is equivalent to the optimization problem in (1) is strongly convex with parameter proportional to  $\sigma$ . Then via standard stochastic gradient decent analysis (e.g., section 3.1 in Lacoste-Julien et al. (2012)), we obtain:

$$\frac{1}{t} \sum_{j=1}^t \left( \frac{1}{2N} \sum_{i=1}^N \|\mathbf{W}_j \mathbf{g}_i - \mathbf{y}_i\|_2^2 \right) - \frac{1}{2N} \sum_{i=1}^N \|\mathbf{W}^* \mathbf{g}_i - \mathbf{y}_i\|_2^2 \leq \mathcal{O}\left(\frac{\log t}{\sigma t}\right) = \tilde{\mathcal{O}}(\sigma^{-1} t^{-1}). \quad (3)$$

Therefore, to reach  $\epsilon$  optimization gap, we just need to set  $t = \tilde{\mathcal{O}}(\sigma^{-1} \epsilon^{-1})$ .  $\square$